Earthquake-induced rotation and settlement of building foundations

M. D. L. Millen[1], M. Cubrinovski[1], S. Pampanin[1] and A. Carr[1]

[1]Department of Civil and Natural Resources Engineering, University of Canterbury, email: maxim.millen@pg.canterbury.ac.nz

ABSTRACT

The recent embrace of a performance-based design (PBD) approach for the design of buildings has increased the need to more rigorously quantify the behaviour of both the structure and the foundation. To ensure suitable foundation performance, the engineer needs tools to both predict the expected level of transient and permanent deformations and control these deformations within the design specifications. There are several experimental tests providing evidence of correlation between residual rotation, peak rotation and axial load, as well as for soil-foundation-structure interaction (SFSI) - induced settlement. However many of these tests use synthetic ground motions or the recorded data is difficult to interpret due to testing in harsh centrifugal conditions.

This paper provides expressions for the expected level of residual foundation rotation and SFSI-induced settlement based on the peak foundation rotation and foundation axial load. The curves were developed from results of an extensive parametric study using an experimentally validated modelling technique, employing a macro soil-foundation interface element and an elastic single-degree-of-freedom structure.

The derivations of the relationships between residual rotation and peak rotation, and SFSI-induced settlement and peak rotation are shown and their dependency on the ratio of applied static axial load to static axial load capacity is examined.

Keywords: Soil-foundation-structure interaction, Performance-based design, residual behaviour

1 INTRODUCTION

A performance-based design methodology requires designers to control the levels of deformations in the structure for the given design loads. The peak transient deformations are of interest in controlling collapse and damage to non-structural elements, while the residual deformations indicate the possibility of repairing the structure itself. There are several empirical equations available for predicting the residual drift of the super-structure for a given peak drift and a governing hysteretic behaviour (eg. Ruiz-Garcia and Miranda, 2006). To have a comprehensive performance-based design the same approach is needed for the foundation deformations.

Early experimental tests at the University of Auckland (Taylor and Williams, 1979) involved rocking foundations under constant axial load on clay and sand. The findings showed that settlement was dependent on the number of cycles, with five cycles at 0.035 rad resulting in a settlement of 0.2% of the footing width. It was recommended that footings should be designed with large factors of safety to prevent large settlements during rocking. Work by Gajan et al. (2005) developed relationships for settlement based on the footing rotation during each cycle from slow cyclic tests and dynamic excitation. In this work the axial load ratio (defined as the ultimate vertical capacity over the applied vertical load), the peak footing rotation and the relative density were all recognised as important parameters relating to settlement. Deng et al. (2012) developed relationships between the settlement and the cumulative plastic rotation (defined as the sum of all the rotations that exceeded a threshold) based on slow cyclic and dynamic centrifuge tests. The research also recognised the axial load as an important parameter.

The recent emergence of a 'weak foundation, strong super-structure' design philosophy or 'shared ductility' between the super-structure and foundation has prompted engineers to question what level of foundation deformations are acceptable. Should foundation uplift be prevented as suggested in many codes around the world? If large transient deformations in the foundation are allowed for, will large residual settlements and residual rotations occur? This paper addresses these questions, not necessarily to advocate for a 'weak foundation, strong super-structure' design approach, but to provide engineers with a tool so that they can check the residual deformations of their foundations, regardless of their design philosophy.

1.1 Mechanisms of foundation rotation

Foundation rotation can be considered as three separate mechanisms: elastic rotation, foundation

uplift and soil yielding (Figure 1). The elastic rotation is a linear elastic mechanism, where the rotation is fully recoverable and the elastic stiffness comes from the footing dimensions, initial shear modulus and Poisson's ratio of the soil. The uplift mechanism is a non-linear elastic mechanism, whereby the deformation is fully recoverable but the rotational stiffness reduces as uplift occurs due to a geometric non-linearity. The soil yielding mechanism is a non-linear inelastic mechanism, whereby the rotation is not recoverable and the stiffness changes as the soil yields.

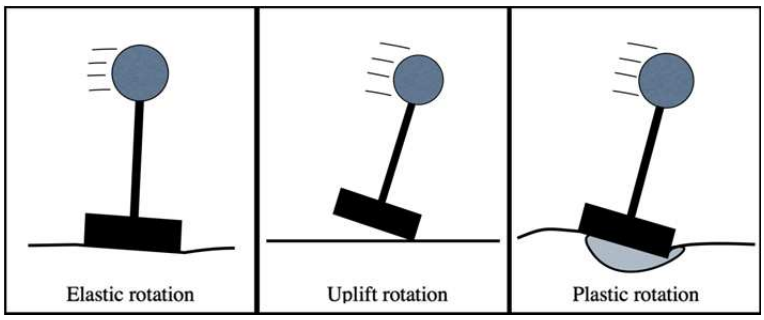

Figure 1. Mechanisms of foundation rotation

Each of these mechanisms contributes different amounts of rotation depending on the level axial load and amount of rotation. The elastic rotation is the biggest contributor for small levels of rotation, while for large rotations, heavily loaded footings are dominated by soil yielding and lightly loaded footings are mainly affected by uplift. Although each mechanism influences the other, this mechanism approach provides a convenient explanation for why the level of residual rotation may be dependent on both the level of rotation and the axial load. The level of axial load can be considered in a normalised form using the axial load ratio ($\widehat{N}$), which is equal to the static factor of safety against bearing capacity failure.

1.2 Mechanisms of settlement

A mechanism approach can also be applied to the prediction of settlement. Two mechanisms contribute to settlement; static settlement and soil-foundation-structure interaction (SFSI) induced settlement. The static component can be considered as the settlement from the compressibility of the soil under the applied gravity loads and will not be discussed any further in this paper. The SFSI-induced settlement occurs due to a shakedown of the foundation into the soil through subsequent cycles of irrecoverable soil yielding through rotation (Figure 2). Based on mechanics it can be seen that a larger axial load leads to a larger amount of yielding for an equivalent level of rotation. Thus the foundation rotation and axial load ratio are both significant parameters in SFSI-induced settlement as was recognised in previous studies (Gajan et al. 2005, Deng et al. 2012).

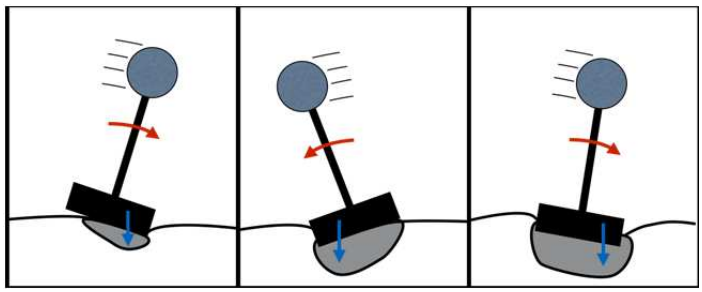

Figure 2. SFSI-induced settlement

2 OBJECTIVES

This paper provides expressions for the expected level of residual foundation rotation and SFSI-induced settlement based on the peak foundation rotation and foundation axial load ratio. The curves were developed from results of an extensive parametric study using an experimentally validated modelling technique, employing a macro soil-foundation interface element and an elastic single-degree-of-freedom structure.

3 PROCEDURE

There are several experimental tests providing evidence of correlation between residual rotation, peak rotation and axial load, as well as for SFSI-induced settlement. However many of these tests use synthetic ground motions or the recorded data is difficult to interpret due to testing in harsh centrifugal conditions. The limited number of testing configurations also makes it difficult to assess the influence of a wide range of parameters. The use of an experimentally validated numerical simulation technique allowed the authors to investigate the relationships between the residual parameters and the peak rotation for a wide range of building and foundation parameters.

3.1 Numerical model setup

The numerical model used in this study consisted of a lumped mass super-structure (M_{ss}) attached to a soil-foundation interface element (Figure 3a). The super-structure was modelled elastically with a horizontal linear dashpot (C_{ss}) set at 3% of critical damping between the foundation and the super-structure. The vertical displacement from the super-structure was slaved to the foundation node providing a perfectly rigid super-structure axial stiffness. The foundation mass (M_f) was modelled with horizontal and vertical masses. The foundation radiation damping was modelled with horizontal (C_{VV}), vertical (C_{NN}) and rotational (C_{MM}), linear dashpots between the foundation and surrounding soil based on the radiation damping equations from Gazetas (1991). The initial stiffnesses (K_{VV}, K_{NN}, K_{MM}) for the soil-foundation element model were based off the stiffnesses suggested in Gazetas (1991), where for embedded foundations the contact area of the sidewalls was assumed to be zero as the numerical model was developed for shallow foundations on the surface. The modification to the stiffnesses due to uplift was captured using the uplift formulation from Chatzigogos (2008). The uplift model has the advantage of capturing the vertical displacement of the centre of the footing, allowing for the vertical inertia and damping to contribute to the behaviour. The soil yielding was modelled using the plasticity model and model parameters from Figini (2012). The plasticity model uses a bounding surface and vertical mapping rule and it has been experimentally validated to reasonably accurately capture the rotational and settlement behaviour at small levels of rotation (Figini, 2012). The foundation capacity (N_{cap}) was determined based on the shallow foundation bearing capacity equations from Salgado (2008). P-delta effects were considered in the analysis. All analyses were carried out using the non-linear time history analysis software Ruaumoko3D (Carr, 2013).

3.2 Experimental validation

The numerical model was calibrated and validated against a model bridge pier structure from the fifth centrifuge experiment (LJD03) from the NEES project: “Innovative Economical Foundations with Improved Performance that is Less Sensitive to Site Conditions” (Deng and Kutter, 2010). The model bridge pier is shown in Figure 3b. A summary of the modelling parameters used to capture the experimental behaviour is shown in Table 1.

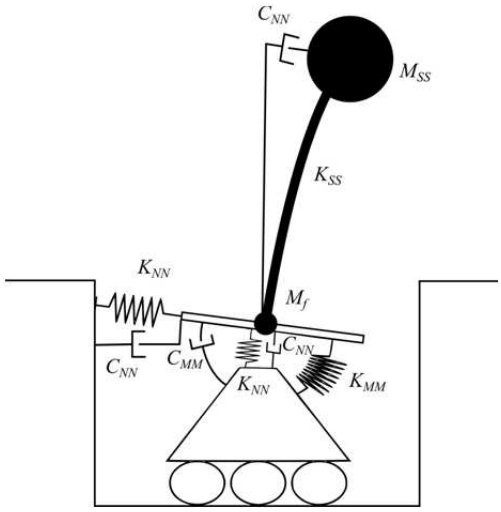

Figure 3a. Numerical SFSI model

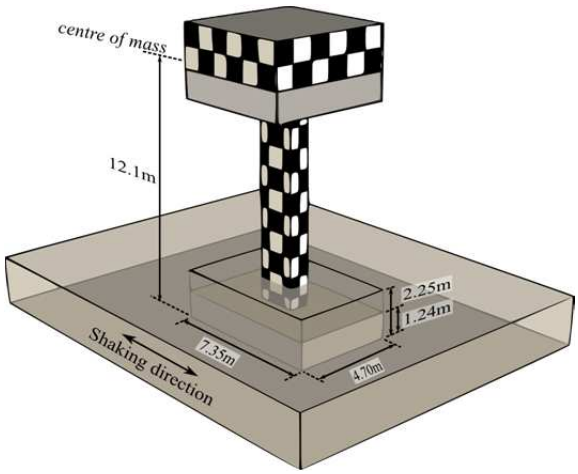

Figure 3b. Experimental test setup (Deng and Kutter, 2010)

Table 1: Input parameters for numerical simulation of experiment by Deng and Kutter (2010)

Parameter	Value	Parameter	Value
Pier height	12.1 m	Footing axial load capacity (N_{cap})	68.0 MN
Deck weight (M_{SS})	632 T	Vertical radiation damping (C_{NN})	13.8 MNs/m
Fixed base period (T_{SS})	1.2 s	Horizontal radiation damping (C_{VV})	8.55 MNs/m
Super-structure damping	3%	Rotational radiation damping (C_{MM})	21.8 MNms
Footing length	7.35 m	Uplift limit factor (α)	5
Footing width	4.70 m	Uplift stiffness factor (ε)	0.65
Footing depth	1.24 m	Uplift stiffness factor (δ)	0.75
Footing embedment	2.24 m	Uplift stiffness factor (γ)	1.5
Footing mass	79 T	Uplift plasticity factor (ζ)	1.5
Soil initial stiffness (G_{max})	30 MPa	Bounding surface shear parameter (μ)	0.469
Poisson's ratio (ν)	0.3	Bounding surface moment parameter(ψ)	0.48
Soil density (ρ)	1.67 T/m^3	Bounding surface shape parameter (ξ)	0.95
Friction angle (φ)	32	Plasticity modulus factor ($p1$)	0.4
Relative density (Dr)	38%	Reload stiffness factor ($p2$)	1
Vertical stiffness (K_{NN})	603 MN/m	Plastic potential shear parameter (λ)	2.5
Horizontal stiffness (K_{VV})	447 MN/m	Plastic potential moment parameter(χ)	3
Rotational stiffness (K_{MM})	6330 MNm		

The results of two of the validation tests are shown in Figures 4a and 4b, where the deck acceleration is the total acceleration, the deck rotation is the rotation of the deck relative to horizontal and the footing moment is the moment determined from the inertia and measured accelerations. The footing rotation is the footing rotation relative to horizontal and the footing settlement is the settlement relative to the ground surface. The numerical model over predicts the high frequency content of the deck movement as seen in the peak acceleration plots but captures the deck and footing rotations reasonably well. The footing moment demand was captured realistically by the model using the uplift and plasticity formulations. The transient settlements from the experiment were not accurately measured, however, the model captured the general trend of the residual settlements from both motions but over predicted the settlement from motion 11 because the model did not account for the densification of the soil under footing from multiple motions. This experimental validation, along with others from Figini (2012) and Chatzigogos (2010), provides some confidence in the model to predict peak and residual foundation deformations.

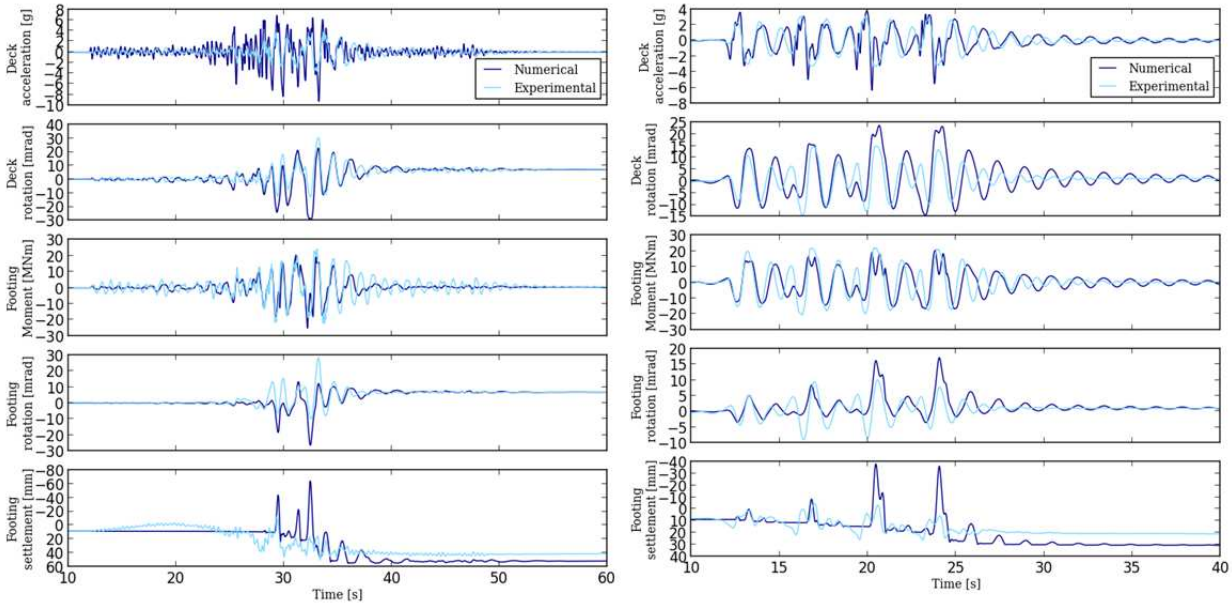

Figure 4. Numerical versus experimental comparison of bridge pier test (a - left) Motion 7 (b - right) Motion 10) – Experimental data from Deng and Kutter (2010)

3.3 Parametric study

The parametric study was an extension of the model used in the above experimental validation, where the input parameters in Table 2 were varied to reflect the range of realistic building/soil types where

SFSI may be of interest. Table 2 describes the range and limitations on the parameters, while Equation 1 provides a limit on the length of foundation perpendicular to axis of foundation rotation (L) based on the expected over-turning moment, foundation shear and the foundation capacity from work by Nova and Montrasio (1991). The foundations were sized to so that the expected moment demand would be approximately the moment capacity, while the (± 0.125) term provides a random variation to the foundation length in an attempt to remove any bias on the results from the imposed limitation.

Table 2: Input parameters for parametric analysis

Parameters	Range
Shear wave velocity (V_s)	$100 \leq V_s \leq 360\ m/s$
Soil mass density (ρ_s)	$1.6 \leq \rho_s \leq 1.9\ (t/m3)$
Poisson's ratio (v)	$v = [0.2, 0.3]$
Friction angle (ϕ)	$30 \leq \phi \leq 40\ degrees$
Fixed base period (T_{SS})	$0.3 \leq T_{SS} \leq 1.8\ s$
Effective height (H)	$\max(2, 9.1T_{SS}^{1.33}) \leq H \leq \min(20, 26.8T_{SS}^{1.33})$
Foundation to super-structure mass ratio ($\bar{m}$)	$0.05 - 0.15$
Design hazard factor (Z)	$Z = 0.4$ for use in NZS 1170.5:2004
Spectral acceleration (S_a)	$S_a = f(T_{SS}, Z, N = 1, R = 1)$ from NZS 1170.5:2004
Axial load ratio ($\widehat{N}$)	$\widehat{N} = [1.5, 2, 5, 20]$
Length of foundation perpendicular to axis of rotation (L)	$\max\left(1.0, \frac{H}{5}\right) \leq L = Eq\ 1 \leq \min(20.0, \mathrm{H}/2)$
Length of foundation parallel to axis of rotation (W)	$0.5L \leq W \leq L$
Foundation embedment (D)	$0 \leq D \leq 0.2L$
Axial load capacity (N_{max})	$N_{max} = f(\phi, \rho_s, L, W, D)$ Salgado (2008)
Vertical weight (N)	$N = N_{max}/\widehat{N}$
Super-structure seismic mass (M_{SS})	$\frac{N}{9.8(1+\bar{m})}$
Footing mass (M_f)	$M_{SS}\bar{m}$
Structural stiffness (K_{SS})	$K_{SS} = 4\pi^2 M_{SS}/T_{SS}^2$

$$L = \frac{S_a\, H_{eff}}{(1+\bar{m})\sqrt{\left(1-\frac{1}{\widehat{N}}\right)^2 - \left(\frac{3\, S_a}{\tan\phi}\right)^2}}\,(0.75 \pm 0.125) \quad (1)$$

The plasticity and uplift model parameters were taken to be the same as those in Table 1. The above parameters were sampled using a stratified sampling technique to generate 180 buildings with a more uniform distribution of the parameters than that of a Monte Carlo simulation.

3.4 Input ground motions

The input motions were selected from the NGA database to minimise the normalised sum of the squared residuals for the NZS 1170.5 site class C spectrum between the periods of 0.2s to 2.5s. Fifteen ground motions were selected and scaled for a hazard level of 0.40g $\pm$ 0.1g, the $\pm$ 0.1g was a random scale factor applied to the records to produce a scatter in the peak rotation values. The spectra (scaled to 0.40g) of the selected ground motions are shown in Figures 5a and 5b and the record data is shown in Table 3.

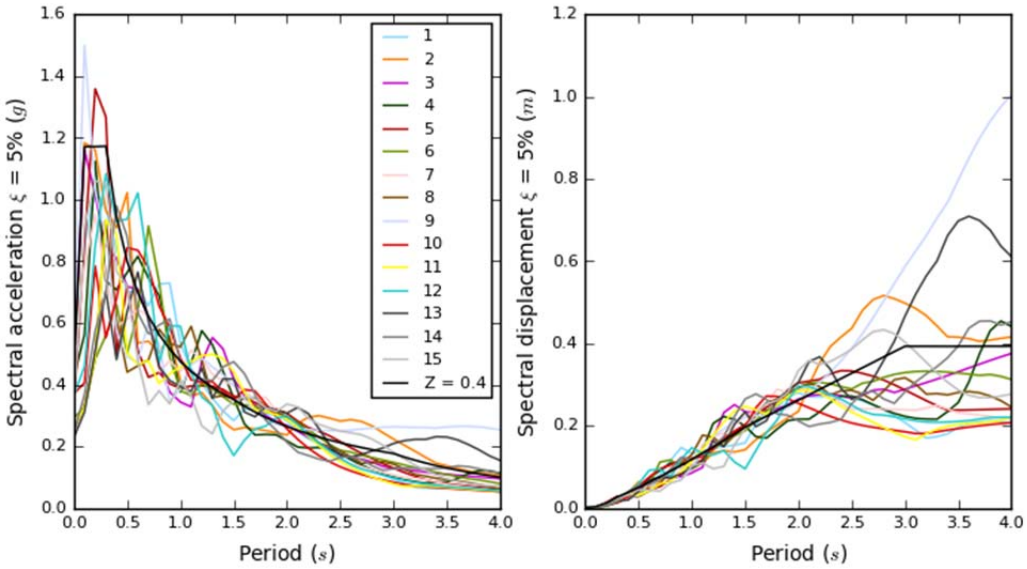

Figure 5. a) Acceleration response spectra and b) Displacement response spectra of selected ground motions

Table 3: Selected ground motions used in parametric analysis

ID	RecName	SF	Event	Year	Station	Mw	PGA (g)	Soil	R (km)
1	NGA0179_1	0.98	Imperial Valley-06	1979	El Centro Array #4	6.5	0.48	D	27.1
2	NGA0180_1	1	Imperial Valley-06	1979	El Centro Array #5	6.5	0.52	D	27.8
3	NGA0183_1	0.94	Imperial Valley-06	1979	El Centro Array #8	6.5	0.56	D	28.1
4	NGA0721_1	1.22	Superstition Hills-02	1987	El Centro Imp. Co. Cent	6.5	0.44	D	35.8
5	NGA0767_2	1.03	Loma Prieta	1989	Gilroy Array #3	6.9	0.38	D	31.4
6	NGA0778_1	1.1	Loma Prieta	1989	Hollister Diff. Array	6.9	0.30	D	45.1
7	NGA0802_1	0.99	Loma Prieta	1989	Saratoga - Aloha Ave	6.9	0.50	C	27.2
8	NGA0803_1	1.02	Loma Prieta	1989	Saratoga - W Valley Coll.	6.9	0.27	C	27
9	NGA0879_1	0.81	Landers	1992	Lucerne	7.3	0.59	C	44
10	NGA1119_1	0.54	Kobe, Japan	1995	Takarazuka	6.9	0.37	D	38.6
11	NGA1158_2	0.75	Kocaeli, Turkey	1999	Duzce	7.5	0.27	D	98.2
12	NGA1197_1	0.57	Chi-Chi, Taiwan	1999	CHY028	7.6	0.37	C	32.7
13	NGA1462_2	1.23	Chi-Chi, Taiwan	1999	TCU	7.6	0.23	C	36.2
14	NGA1504_2	0.79	Chi-Chi, Taiwan	1999	TCU067	7.6	0.26	C	28.7
15	NGA1633_2	0.76	Manjil, Iran	1990	Abbar	7.4	0.38	C	40.4

4 RESULTS

In Figure 6 the parametric analysis results show that clear relationships exist between the two residual foundation parameters and the peak rotation with the best fit of the data shown along with the 95% confidence interval based on ϵ =1.67 times the standard deviation, for Equations 2-4. The axial load ratio had an influence on the expected settlement as anticipated, however its influence was limited to only the case of axial load ratio of two (Figure 6 b). At axial load ratios greater than two there was no quantifiable modification to the settlement due to the axial load ratio (Figure 6 a). The results were analysed using multiple parameter regression analysis, however the additional axial load terms as well as the 5-95% significant duration provided no physically significant modifications to the results. The soil stiffness was also examined as a potentially influential parameter, however it was significantly correlated with the peak rotation and the peak rotation provided a better fit to the data. The few data points providing smaller than expected settlement values were the cause of significant residual rotations at the end of the earthquake. The residual rotation was significant enough to cause the centre of the foundation to be lifted even though the compression edge may have settled significantly. The few results with higher than expected settlements were due to considerable moment-shear force interaction on the footing causing a significant reduction in moment capacity and conditions close to failure, the settlement values predicted for these cases are very sensitive to the modelling

assumptions. Equations 2 and 3 provide the relationships between the peak foundation rotation ($\theta_{f,p}$) and the SFSI-induced settlement (Δ) normalised by the foundation length (L).

$$\hat{N} = 2: \quad \frac{\Delta}{L} = 10^{(-1.17+\epsilon)}\theta_{f,p}^{0.766} \quad \text{standard deviation = 0.16} \tag{2}$$

$$\hat{N} \geq 3: \quad \frac{\Delta}{L} = 10^{(-1.16+\epsilon)}\theta_{f,p}^{0.810} \quad \text{standard deviation = 0.20} \tag{3}$$

The axial load ratio showed no significant influence on the expected level of residual rotation for the given tests, however it may still be influential at considerably higher and lower axial load ratios and for a more consistent design procedure. The residual rotation showed a very large scatter, especially the lower values. This sort of behaviour is expected as an earthquake provides a cyclic load to the system and although peak rotations may be very high, the cyclic loading provides a restoring force in the opposite direction to reduce permanent deformations. The maximum residual rotation for a given peak rotation did show a clear trend. The maximum residual rotations closely follow the increase in peak rotation especially after a drift of 0.001 rad. The residual rotation is slightly less than the peak rotation as some elastic energy is stored during rotation. The maximum residual rotation can be predicted using the 95% single sided confidence interval determined from regression analysis. Equation 4 below provides the relationship between the peak rotation and the residual rotation for all axial load cases. The significant duration and soil stiffness were again considered in a multiple parameter regression, but provided no quantifiable modification to the relationships.

$$\theta_{f,r} = 10^{(-1.32+\epsilon)}\theta_{f,p}^{0.934} \quad \text{standard deviation = 0.52} \tag{1}$$

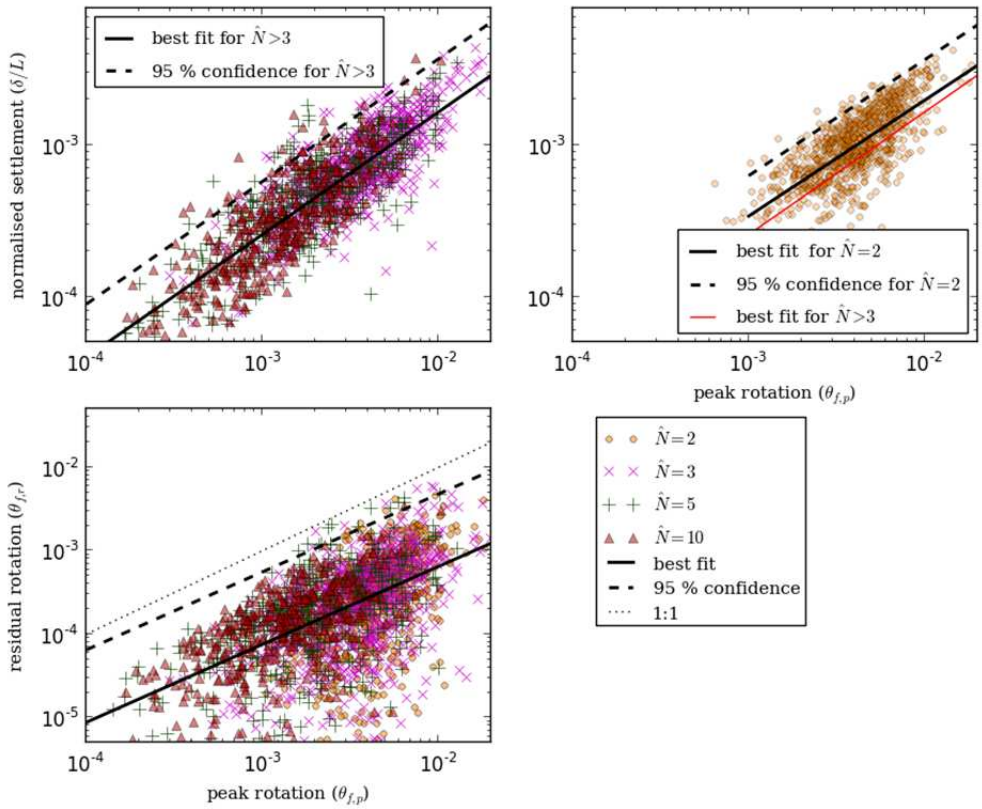

Figure 6. (a - top left) Results and regression relationship between normalised settlement and peak rotation for $\hat{N} \geq 3$ (b - top right) Results and regression relationship between normalised settlement and peak rotation for $\hat{N} = 2$ (c - bottom left) Results and regression relationship between residual rotation and peak rotation for all axial load conditions

5 DISCUSSION

This paper demonstrates that relationships exist between the peak foundation rotation and the foundation residual deformations (foundation residual rotation and SFSI-induced settlement). The

mechanics-based approach to foundation rotation and SFSI-induced settlement suggests that both peak rotation and axial load ratio may be influencing parameters for residual deformation. The parametric study confirmed that a relatively strong relationship between the peak rotation and residual deformation exists, however the axial load ratio provided significant modification to the SFSI-induced settlement only for an axial load ratio of two, and no noticeable modification to the residual settlement for higher ratios. The large scatter in the results from the parametric study reflects the uncertainties in the estimation of residual parameters and therefore parametric studies based on a more rigorous design procedure and scaling of earthquake motions may be needed to provide better estimates and constraints. The prediction of residual foundation deformations also includes the additional uncertainty associated with the prediction of the peak foundation rotation.

While these curves provide an indication on the level of settlement and residual deformation that can be expected, the parametric study and consequent regression analyses have been based on the results from a single set of experimental tests conducted on Nevada Sand, hence the results for other soil conditions may vary significantly. The results are also limited by the relatively simple numerical models used and the limited range of parameters considered in this study.

6 CONCLUSION

This paper presents relationships between the peak foundation rotation and soil-foundation-structure interaction induced settlement and residual foundation rotation. The importance of the axial load ratio was explained and investigated in the development of the presented relationships. The relationships were developed from statistical regression of results from a parametric numerical study using an experimentally validated modelling technique. The derived relationships provide an indication of the expected level of residual deformations at the foundation level due to soil-foundation-structure interaction.

7 ACKNOWLEDGEMENTS

The authors would like to acknowledge the generosity of Deng, L. and Kutter, B. L. for the use of the experimental data from the fifth centrifuge experiment (LJD03) from the NEES project: “Innovative Economical Foundations with Improved Performance that is Less Sensitive to Site Conditions” (Deng and Kutter, 2010).

REFERENCES

Carr, A. J. (2012). “Ruaumoko, Nonlinear FEM Computer Program.” Department of Civil Engineering, University of Canterbury, New Zealand.

Deng, L. and Kutter, B. L. (2010). SEISMIC PERFORMANCE OF BRIDGE SYSTEMS WITH ROCKING FOUNDATIONS: CENTRIFUGE DATA REPORT FOR LJD03. Technical report.

Deng, L., Kutter, B. L. and Kunnath, S. K. (2012). “Centrifuge Modeling of Bridge Systems Designed for Rocking Foundations.” Journal of Geotechnical and Geoenvironmental Engineering 138(3), 335–344.

Dep. Building & Housing (2011). “Compliance Document for New Zealand Building Code Clause B1 Structure.” pp. 1–88.

Figini, R., Paolucci, R. and Chatzigogos, C. T., (2012). “A macro-element model for non-linear soil-shallow foundation-structure interaction under seismic loads: theoretical development and experimental validation on large scale tests.” Earthquake Engineering & Structural Dynamics 41(3), 475–493.

Gazetas 1991 ** Foundation vibrations (include reference)

Gajan, S., Kutter, B. L., Phalen, J. D., Hutchinson, T. C., and Martin, G. R., (2005). “Centrifuge modeling of load-deformation behavior of rocking shallow foundations.” Soil Dynamics and Earthquake Engineering 25(7-10), 773–783.

Moghaddasi, M., Cubrinovski, M., Chase, J. G., Pampanin, S., and Carr, A. J. (2012). “Stochastic Quantification of Soil-Shallow Foundation-Structure Interaction.” Journal of Earthquake Engineering 16(6), 820–850.

Nova, R. and Montrasio, L. (1991). “Settlements of shallow foundations on sand.” Géotechnique 41(2), 243–256.

NZS 1170.5:2004 (2004, August). Structural Design Actions - Part 5: Earthquake actions- New Zealand.

Pecker, A. (2007). Soil Structure Interaction. In *Advanced Earthquake Engineering Analysis*, pp. 1–10. Springer.

Ruiz-Garcia, J. and Miranda, E. (2006). “Residual displacement ratios for assessment of existing structures.” Earthquake Engineering & Structural Dynamics 35(3), 315–336.

Salgado, R. (2008). “Shallow foundations: Limit bearing analysis.” The Engineering of Foundations. pp. 409. McGraw Hill New York.

Taylor, P. W. and Williams, R. L. (1979). “Foundations for capacity designed structures.” Bulletin of the New Zealand Society for Earthquake Engineering 12.